

# PyCARL: A PyNN Interface for Hardware-Software Co-Simulation of Spiking Neural Network

Adarsha Balaji<sup>1</sup>, Prathyusha Adiraju<sup>2</sup>, Hirak J. Kashyap<sup>3</sup>, Anup Das<sup>1,2</sup>,  
Jeffrey L. Krichmar<sup>3</sup>, Nikil D. Dutt<sup>3</sup>, and Francky Catthoor<sup>2,4</sup>

<sup>1</sup>Electrical and Computer Engineering, Drexel University, Philadelphia, USA

<sup>2</sup>Neuromorphic Computing, Stichting Imec Nederlands, Eindhoven, Netherlands

<sup>3</sup>Cognitive Science and Computer Science, University of California, Irvine, USA

<sup>4</sup>ESAT Department, KU Leuven and IMEC, Leuven, Belgium

Correspondence Email: anup.das@drexel.edu, jkrichma@uci.edu, Francky.Catthoor@imec.be

**Abstract**—We present PyCARL, a PyNN-based common Python programming interface for hardware-software co-simulation of spiking neural network (SNN). Through PyCARL, we make the following two key contributions. First, we provide an interface of PyNN to CARLsim, a computationally-efficient, GPU-accelerated and biophysically-detailed SNN simulator. PyCARL facilitates joint development of machine learning models and code sharing between CARLsim and PyNN users, promoting an integrated and larger neuromorphic community. Second, we integrate cycle-accurate models of state-of-the-art neuromorphic hardware such as TrueNorth, Loihi, and DYNAPSE in PyCARL, to accurately model hardware latencies that delay spikes between communicating neurons and degrade performance. PyCARL allows users to analyze and optimize the performance difference between software-only simulation and hardware-software co-simulation of their machine learning models. We show that system designers can also use PyCARL to perform design-space exploration early in the product development stage, facilitating faster time-to-deployment of neuromorphic products. We evaluate the memory usage and simulation time of PyCARL using functionality tests, synthetic SNNs, and realistic applications. Our results demonstrate that for large SNNs, PyCARL does not lead to any significant overhead compared to CARLsim. We also use PyCARL to analyze these SNNs for a state-of-the-art neuromorphic hardware and demonstrate a significant performance deviation from software-only simulations. PyCARL allows to evaluate and minimize such differences early during model development.

## I. INTRODUCTION

Advances in computational neuroscience have produced a variety of software for simulating spiking neural networks (SNNs) [1], which facilitates machine learning application development with neurobiological details. Examples of these simulators include NEURON [2], NEST [3], PCSIM [4], and Brian [5]. These simulators model neural functions at various levels of detail and therefore have different requirements for computational resources. CARLsim 4.0 [6], the latest version of the SNN simulation library CARLsim [7], facilitates parallel simulation of large SNNs using CPUs and multi-GPUs, simulates multiple compartment models, 9-parameter Izhikevich and leaky integrate-and-fire (LIF) spiking neuron models, and integrates the fourth order Runge Kutta (RK4) method for improved numerical precision. CARLsim’s support for built-in biologically realistic neuron, synapse, current and emerging learning models and continuous integration and testing, make it an easy to use and powerful simulator of

biologically-plausible neural network models. Benchmarking results demonstrate simulation of 8.6 million neurons and 0.48 billion synapses using 4 GPUs and up to 60x speedup for multi-GPU implementations over a single-threaded CPU implementation, making CARLsim well-suited for simulating large-scale SNN models [6].

To facilitate faster application development and portability across research institutes, a common Python programming interface called PyNN has been proposed [8]. PyNN provides a high-level abstraction of SNN models, promotes code sharing and reuse, and provides a foundation for simulator-agnostic analysis, visualization and data-management tools. Many SNN simulators now support interfacing with PyNN. Examples include PyNEST [9], PyPCSIM [10], and Brian 2 [11].

**Contribution 1:** Currently, no interface exists between the CARLsim simulator, which is implemented in C++ and PyNN. Therefore, applications developed in PyNN cannot be analyzed using CARLsim and conversely, PyNN-based applications cannot be analyzed using CARLsim. This creates a big gap between these two research communities. Our objective is to bridge this gap and create an integrated neuromorphic research community, facilitating joint developments of machine learning models and efficient code sharing. Figure 1 illustrates the standardized application programming interface (API) architecture in PyNN. Brian 2 and PCSIM, which are native Python implementations, employ a direct communication via the `pynn.brian` and `pynn.pcsim` API calls, respectively. NEST, on the other hand, is not a native Python simulator. So, the `pynn.nest` API call first results in a code generation to the native SLI code, a stack-based language derived from PostScript. The generated code is then used by the Python interpreter PyNEST to simulate an SNN application utilizing the backend NEST simulator kernel. Figure 1 also shows our proposed interface for CARLsim, which is exposed via the new `pynn.carlism` API in PyNN. We describe this interface in details in Section III and analyze its performance in Sec. VI.

On the hardware front, neuromorphic computing [12] has shown significant promise to fuel the growth of machine learning, thanks to low-power design of the underlying computing circuits, distributed implementation of computing and storage, and novel technology integration in the form of non-volatile memories. In recent years, several spiking neuromorphic ar-

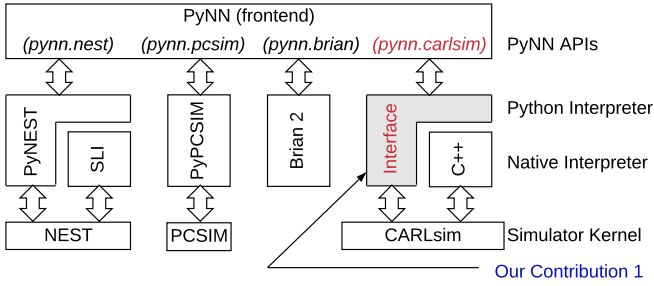


Fig. 1: PyNN standardized API architecture and our proposed pynn-to-carlsim interface.

chitectures are designed: DynapSE [13], TrueNorth [14] and Loihi [15]. Unfortunately, due to non-zero latency of different hardware components, spikes between communicating neurons suffer non-deterministic delays, impacting performance of the SNN when executed on these hardware platforms.

**Contribution 2:** Currently, no PyNN-based simulators estimate performance of an SNN on a target neuromorphic platform. Therefore, performance estimated using PyNN can be different from performance obtained when the SNN is executed on the hardware. Our objective is to estimate this performance difference, allowing users to optimize their machine learning model to meet the desired performance in hardware. Figure 2 shows our proposed carlsim-to-hardware interface to estimate SNN performance in hardware. This interface is designed to model state-of-the-art neuromorphic hardware such as TrueNorth, Loihi, and DynapSE at a cycle-accurate level using the output generated from the proposed pynn-to-carlsim interface (see Figure 1). We describe this cycle-accurate hardware model in details in Section IV.

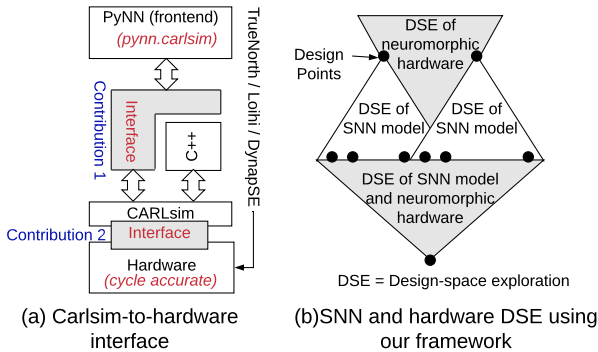


Fig. 2: (a) Our proposed interface to estimate SNN performance on neuromorphic hardware and (b) design space exploration (DSE) based on this contribution.

In Section VI, we show that accuracy of the hand written digit recognition application on a state-of-the-art neuromorphic hardware can be 22% lower than what is estimated using software simulations. PyCARL allows to estimate such performance deviation early during model development. Users can then readily perform design space exploration (DSE) with different SNN topologies and hardware configurations to optimize both model performance such as accuracy and hardware performance such as latency, energy, and throughput. We illustrate this SNN-hardware DSE in Figure 2(b).

**Summary:** To summarize, our comprehensive framework, which we call PyCARL, allows CARLsim based detailed

software simulations, hardware-software co-simulations, and neuromorphic design-space explorations, all from a common PyNN frontend, allowing extensive portability across different research institutes. By using cycle-accurate models of state-of-the-art neuromorphic hardware, PyCARL allows users to perform hardware exploration and performance estimation early during application development, accelerating the neuromorphic product development cycle.

## II. PYCARL INTEGRATED FRAMEWORK

Figure 3 shows a high-level overview of our integrated framework PyCARL, based on PyNN. An SNN model written in PyNN is simulated using the CARLsim backend kernel for the proposed pynn-to-carlsim interface (contribution 1). This generates the first output `snn.sw.out`, which consists of synaptic strength of each connection in the network and precise timing of spikes on these connections. This output is then used in the proposed carlsim-to-hardware interface, allowing simulating the SNN on cycle-accurate models of state-of-the-art neuromorphic hardware such as TrueNorth [14], Loihi [15], and DynapSE [13]. Our cycle-accurate model generates the second output `snn.hw.out`, which consists of 1) hardware-specific metrics such as latency, throughput, and energy, and 2) SNN-specific metrics such as inter-spike interval distortion and disorder spike count (which we formulate and elaborate in Section IV). SNN-specific metrics estimate the performance drop due to non-zero hardware latencies.

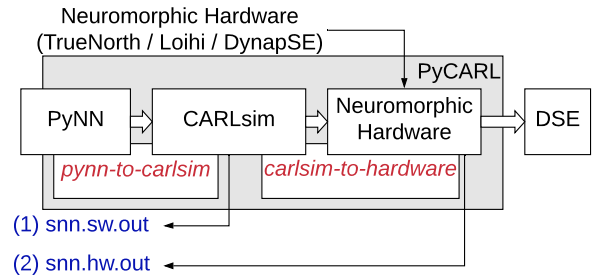


Fig. 3: Our integrated framework PyCARL.

We now describe in details the components of our framework PyCARL. We also show how to use PyCARL to perform design space explorations optimizing hardware metrics.

## III. PYNN-TO-CARLSIM INTERFACE IN PYCARL

Apart from bridging the gap between the PyNN and the CARLsim research communities, the proposed pynn-to-carlsim interface is also significant in the following three ways. First, Python being an interactive language allows users to interact with the CARLsim kernel through command line, reducing the application development time. Second, the proposed interface allows code portability across different operating systems (OSes) such as Linux, Solaris, Windows, and Macintosh. Third, Python being open source, allows distributing the proposed interface with mainstream OS releases, exposing neuromorphic computing to the systems community.

An interface between Python (PyNN) and C++ (CARLsim) can be created using the following two approaches. First, through statically linking the C++ library with a Python interpreter. This involves copying all library modules used in CARLsim into a final executable image by an external program called linker or link editors. Statically linked files

are significantly larger in size because external programs are built into the executable files, which needs to be loaded into the memory every time they are invoked. This increases program execution time. Static linking also requires all files to be recompiled every time one or more of the shared modules change. A second approach is the dynamic linking, which involves placing the names of the external libraries (shared libraries) in the final executable file while the actual linking taking place at run time. Dynamic linking is performed by the operating system through API calls. Dynamic linking places only one copy of shared library in memory. This significantly reduces the size of executable programs, thereby saving memory and disk space. Individual shared modules can be updated and recompiled, without compiling the entire source code again. Finally, load time of shared libraries is reduced if the shared library code is already present in memory. Due to lower execution time, reduced memory usage, and flexibility, we adopt dynamic linking of CARLsim with PyNN.

We now describe the two steps involved in creating the proposed pyinn-to-carlsim interface.

#### A. Step 1: Generating the Interface Binary *carlsim.so*

Unlike PyNEST, which generates the interface binary manually, we propose to use the Simplified Wrapper Interface Generator (SWIG), downloadable at <http://www.swig.org>. SWIG simplifies the process of interfacing high level languages such as Python with low-level languages such as C/C++, preserving the robustness and expressiveness of these low-level languages from the high-level abstraction.

The SWIG compiler creates a wrapper binary code by using headers, directives, macros, and declarations from the underlying C++ code of CARLsim. Figures 4-8 show the different components of the input file *carlsim.i* needed to generate the compiled interface binary file *carlsim.so*. The first component consists of interface files that are treated differently by SWIG and are included using the `%include` directives towards the beginning of the file (Figure 4).

```
// Include interface files if necessary
#include <std_string.i>
#include <std_vector.i>
#include <std_vectora.i>
#include <stl.i>
#include <std_shared_ptr.i>
#include <std_array.i>
```

Fig. 4: Define interface files using the `%include` directive.

The second component consists of declaration of data structures (e.g., vectors) used in the CARLsim implementation (Figure 5) using the `%template` directive.

```
namespace std {
  %template(vectori) vector<int>;
  %template(vectord) vector<double>;
};
```

Fig. 5: Declare CARLsim data structures using the `%template` directive.

The third component is the definition of the main module that can be loaded in Python using the `import` command. This is shown in Figure 6 with the `%module` directive containing pointers to the base class and function definitions.

The fourth component, which we illustrate in Figure 7, consists of enumerated data types defined by the directive `enum`. In this example we show two definitions – 1) the STDP curve and 2) the computing platform.

```
%module carlsim
%{
  /* Put headers and other declarations here */
#include "../CARLsim4/carlsim/interface/inc/carlsim.h"
#include "../CARLsim4/carlsim/interface/inc/carlsim_datastructures.h"
#include "../CARLsim4/carlsim/interface/inc/carlsim_definitions.h"
#include "../CARLsim4/carlsim/interface/inc/callback.h"
%}
}
```

Fig. 6: Main module definition for import in Python.

```
enum STDPCurve {
  EXP_CURVE,
  PULSE_CURVE,
  TIMING_BASED_CURVE,
  UNKNOWN_CURVE
};

enum ComputingBackend {
  CPU_CORES,
  GPU_CORES
};
```

Fig. 7: Enumerated data types using the `enum` directive.

The last component of the input file is the CARLsim class object along with its member functions, which define CARLsim functionalities. We illustrate this in Fig. 8.

```
class CARLsim{
public:
  // creating carlsim object//
  CARLsim(const std::string& netName = "SNN", SimMode
  preferredSimMode = CPU_MODE, LoggerMode loggerMode = USER,
  int ithGPUS = 0, int randSeed = -1);

  ~CARLsim();
  // creating groups and spikegenerator group//
  int createSpikeGeneratorGroup(const std::string& grpName,
  int nNeur, int neurType, int preferredPartition = ANY,
  ComputingBackend preferredBackend = CPU_CORES);

  int createSpikeGeneratorGroup(const std::string& grpName,
  const Grid3D& grid, int neurType, int preferredPartition = ANY,
  ComputingBackend preferredBackend = CPU_CORES);

  int createGroup(const std::string& grpName, int nNeur,
  int neurType, int preferredPartition = ANY,
  ComputingBackend preferredBackend = CPU_CORES);

  int createGroup(const std::string& grpName, const Grid3D& grid,
  int neurType, int preferredPartition = ANY,
  ComputingBackend preferredBackend = CPU_CORES);
};
```

Fig. 8: CARLsim class object.

The major advantage of using SWIG is that it uses a layered approach to generate a wrapper over C++ classes. At the lowest level, a collection of procedural ANSI-C style wrappers are generated by SWIG. These wrappers take care of the basic type conversions, type checking, error handling and other low-level details of C++ bindings. To generate the interface binary file *carlsim.so*, the input file *carlsim.i* is compiled using the swig compiler as shown in Figure 9.

```
~/swig-3.0.12/Examples/python/CARLsim4/carlsim$ swig -c++ -python carlsim.i
```

Fig. 9: Compilation of *carlsim.i* using the SWIG compiler to generate *carlsim.so* interface binary.

#### B. Step 2: Designing PyNN API to Link the Interface Binary *carlsim.so*

We now describe the proposed `pyinn.carlsim` API to link the interface binary *carlsim.so* in PyNN.

The *carlsim.so* interface binary is placed within the sub-package directory of PyNN. This exposes CARLsim internal methods as a Python library using the `import` command as `from carlsim import *`. The PyNN front-end API architecture supports implementing both basic functionalities (common for all backend simulators) and specialized simulator-specific functionalities.

1) *Implementing common functionalities:* PyNN defines many common functionalities to create a basic SNN model. Examples include cell types, connectors, synapses, and electrodes. Figure 10 shows the UML class diagram to create the Izhikevich cell type [16] using the `pynn.carlsim` API. The inheritance relationship shows that the PyNN `standardmodels` class includes the definition of all the methods under the `StandardModelType` class. The Izhikevich model and all similar standard cell types are a specialization of this `StandardModelType` class, which subsequently inherits from the PyNN `BaseModelType` class. Defining other standard components of an SNN model follow similar inheritance pattern using the common internal API functions provided by PyNN.

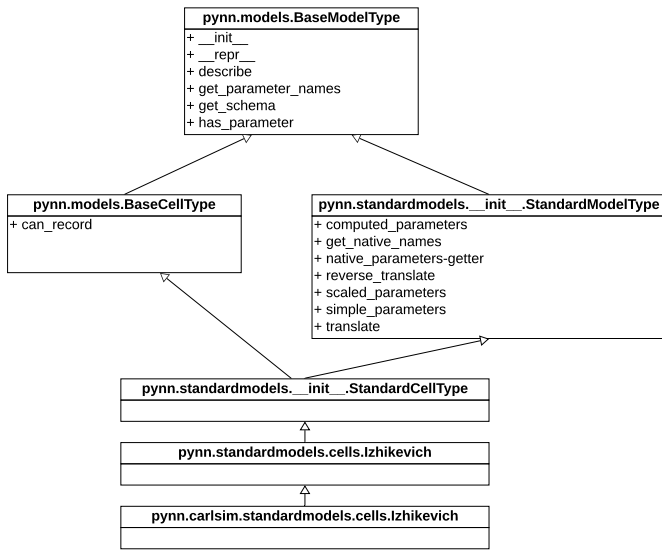


Fig. 10: UML class diagram of Izhikevich cell type showing the relationship with the `pynn.carlsim` API.

2) *Implementing specialized CARLsim functions:* Using the standard PyNN classes, it is also possible to define and expose non-standard CARLsim functionalities.

Figure 11 details the `state` class of CARLsim. The composition adornment relationship between the `state` class of the simulator module and the `CARLsim` class in the `pynn.carlsim` API. The composition adornment means that apart from the composition relationship between the contained class (`CARLsim`) and the container class (`State`), the object of the contained class also goes out of scope when the containing class goes out of scope. Thus, the `State` class exercises complete control over the members of the `CARLsim` class objects. The class member variable `network` of the `simulator.State` class contains an instance of the `CARLsim` object. From Figure 11 it can be seen that the `CARLsim` class consists of methods which can be used for the initial configuration of an SNN model and also methods for running, stopping and saving the simulation. These functions are appropriately exposed to the PyNN by including them in the `pynn.carlsim` API methods, which are created as members of the class `simulator.State`.

Figure 12 shows the implementations of the `run()` and

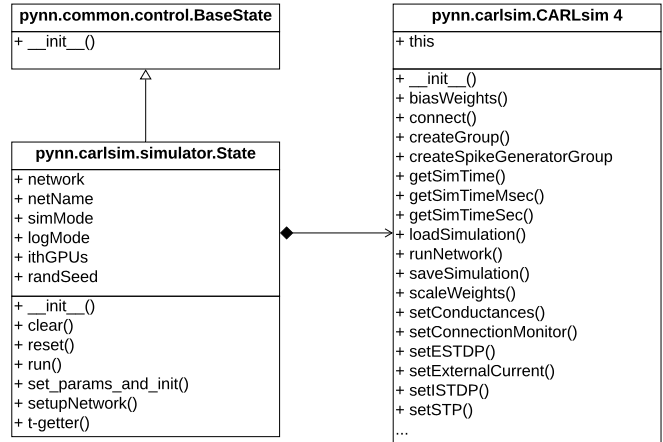


Fig. 11: UML class diagram of simulator state of the `pynn.carlsim` API.

`setupNetwork()` methods in the `simulator.State` class. It can be seen that these methods call the corresponding functions in the `CARLsim` class of the `pynn.carlsim` API. This technique can be used to expose other non-standard CARLsim methods in the `pynn.carlsim` API.

```
def run(self, simtime):
    self.running = True
    nSec = simtime/1000
    nMsec = simtime%1000
    self.network.runNetwork(int(nSec), int(nMsec))

def setupNetwork(self):
    self.network.setupNetwork()
```

Fig. 12: Snippet showing the exposed CARLsim functions in the `pynn.carlsim` API.

### C. Using the Proposed `pynn-to-carlsim` Interface

To verify the integrity of our implementation, Figure 13 shows the source code of a test application written in PyNN. The source code sets SNN parameters using PyNN. A simple spike generation group with 1 neuron and a second neuron group with 3 excitatory Izhikevich neurons are created. The user can run the code in a CPU or a GPU mode by specifying the respective parameters in the command line.

It can be seen from the figure that command line arguments have been specified to receive the simulator specific parameters from the user. This command line parameters can be replaced with custom defined methods in the `pynn.carlsim` API of PyNN or by using configuration files in xml or json format. The application code shows the creation of an SNN model by calling the `get_simulator` method. To use CARLsim back-end, an user must specify “`carlsim`” as the simulator to be used for this script while invoking the Python script, as can be seen in Figure 14. This results in the internal resolution of creating an instance of `CARLsim` internally by PyNN. The returned object (denoted as `sim` in the figure) is then used to access all the internal API methods offering the user control over the simulation.

Figure 15 shows the starting of the simulation by executing the command in Figure 14. As can be seen, the `CPU_MODE` is set by overriding the `GPU_MODE` as no argument was provided in the command and the default mode being `CPU_MODE` was set. The test is being run in the logger



```

from numpy import arange
from pyNN.utility import get_simulator
from pyNN.carlsim import *
import time

# Configure the application (i.e) configure the additional
# simulator parameters

sim, options = get_simulator(("netName", "String for name of
simulation"),
("-gpuMode", "Enable GPU_MODE (CPU_MODE by default)",
{"action": "store_true"}),
{"logMode": "Enter logger mode (USER by default)",
"default": "USER"},
{"ithGPUS", "Number of GPUs"},
{"randSeed", "Random seed"})

logMode = None
ithGPUS = None
randSeed = None

# Validate and assign appropriate options
netName = options.netName

if options.gpuMode:
    simMode = sim.GPU_MODE
else:
    simMode = sim.CPU_MODE

if options.logMode == "USER":
    logMode = sim.USER
elif options.logMode == "DEVELOPER":
    logMode = sim.DEVELOPER

ithGPUS = int(options.ithGPUS)
if (simMode == sim.CPU_MODE and int(ithGPUS) > 0):
    print("Simulation set to CPU_MODE - overriding numGPUS to 0")
ithGPUS = 0

randSeed = int(options.randSeed)

#####
# Start of application code
#####
sim.setup(timestep=0.01, min_delay=1.0, netName = netName, simMode =
simMode, logMode = logMode, ithGPUS = ithGPUS, randSeed = randSeed)
numNeurons = 1

# define the neuron groups
inputCellType = sim.SpikeSourceArray("input", numNeurons,
"EXCITATORY_NEURON" "CUBA")
spike_source = sim.Population(numNeurons, inputCellType)
izhikevichCellType = sim.Izhikevich("EXCITATORY_NEURON", a=0.02,
b=0.2, c=-65, d=6, i_offset=[0.014, 0.0, 0.0])
neuron_group1 = sim.Population(numNeurons, izhikevichCellType)

# connect the neuron groups
connection = sim.Projection(spike_source, neuron_group1,
sim.OneToOneConnector(), receptor_type='excitatory')

# function has to be called before any record function is called.
sim.state.setupNetwork()

# start the recording of the groups
neuron_group1.record('spikes')

# run the simulation for 1000ms
sim.run(1000)
sim.end()

```

Fig. 13: An example application code written in PyNN.

```
~/PyNN/examples$ python test.py carlsim "test" USER 1 42
```

Fig. 14: Executing the test application from command line using CARLsim as the back-end simulator.

mode USER with a random seed of 42 as specified in the command line. From Figure 13, we see that the application is set in the current-based (CUBA) mode, which is also reported during simulation (Fig. 15). The timing parameters such as the AMPA decay time and the GABAB decay times are set in simulation as shown in Figure 13.

In Section VI, we evaluate the memory and timing overhead of this proposed pyNN-to-carlsim interface using both synthetic and realistic applications.

#### D. Generating Output `snn.sw.out`

At the end of simulation, the proposed pyNN-to-carlsim interface generates the following information.

- **Spike Data:** the exact spike times of all neurons in the SNN model and stores them in a 2D spike vector. The

```

Simulation set to CPU_MODE - overriding numGPUS to 0
*****
***** Welcome to CARLsim 4.0 *****
*****
***** Configuring Network *****
Starting CARLsim simulation "test" in USER mode
Random number seed: 42
Running COBA mode:
- AMPA decay time           = 5 ms
- NMDA rise time (disabled) = 0 ms
- GABAA decay time         = 6 ms
- GABAB rise time (disabled) = 0 ms
- GABAB decay time        = 150 ms
Running COBA mode:
- AMPA decay time           = 0 ms
- NMDA rise time (disabled) = 0 ms
- GABAA decay time         = 0 ms
- GABAB rise time (disabled) = 0 ms
- GABAB decay time        = 0 ms

```

Fig. 15: Simulation snippet.

first dimension of the vector is neuron id and the second dimension is spike times. Each element  $spkVector[i]$  is thus a vector of all spike times for the  $i^{\text{th}}$  neuron.

- **Weight Data:** the synaptic weights of all synapses in the SNN model and stores them in a 2D connection vector. The first dimension of the vector is the pre-synaptic neuron id and the second dimension is the post-synaptic neuron id. The element  $synVector[i,j]$  is the synaptic weight of the connection  $(i,j)$ .

The spike and weight data can be used to analyze and adjust the SNN model. They form the output `snn.sw.out` of our integrated framework PyCARL.

## IV. HARDWARE-SOFTWARE CO-SIMULATION IN PYCARL

To estimate the performance impact of executing SNNs on a neuromorphic hardware, the standard approach is to map the SNN to the hardware and measure the change in spike timings, which are then analyzed to estimate the performance deviation from software simulations. However, there are three limitations to this approach. First, neuromorphic hardware are currently in their research and development phase in a selected few research groups around the world. They are not yet commercially available to the bigger systems community. Second, neuromorphic hardware that are available for research have limitations on the number of synapses per neuron. For instance, DynapSE can only accommodate a maximum of 128 synapses per neuron. These hardware platforms therefore cannot be used to estimate performance impacts on large-scale SNN models. Third, existing hardware platforms have limited interconnect strategies for communicating spikes between neurons, and therefore they cannot be used to explore the design of scalable neuromorphic architectures that minimize latency, a key requirement for executing real-time machine learning applications. To address these limitations, we propose to design a cycle-accurate neuromorphic hardware simulator, which can allow the systems community to explore current and future neuromorphic hardware to simulate large SNN models and estimate the performance impact.

### A. Designing cycle-accurate hardware simulator

Figure 16(a) shows the architecture of a neuromorphic hardware with multiple crossbars and a shared interconnect. Analogous to the mammalian brain, synapses of a SNN can be grouped into local and global synapses based on the distance information (spike) conveyed. Local synapses are

short distance links, where pre- and post-synaptic neurons are located in the same vicinity. They map inside a crossbar. Global synapses are those where pre- and post-synaptic neurons are farther apart. To reduce power consumption of the neuromorphic hardware, the following strategies are adopted:

- the number of point-to-point local synapses is limited to a reasonable dimension (size of a crossbar); and
- instead of point-to-point global synapses (which are of long distance) as found in a mammalian brain, the hardware implementation usually consists of time-multiplexed interconnect shared between global synapses.

DynapSE for example, consists of four crossbars, each with 128 pre- and 128 post-synaptic neurons implementing a full 16K (128x128) local synapses per crossbar.

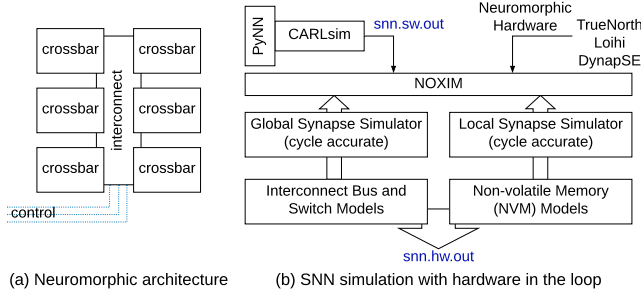


Fig. 16: (a) Neuromorphic architecture and (b) SNN Simulation with hardware in the loop.

Since local synapses map within the crossbar, their latency is fixed and can be estimated offline. However, the global synapses are affected by variable latency introduced due to time multiplexing of the shared interconnect at runtime. Figure 16(b) shows the proposed framework for SNN simulation with hardware in the loop. The `snn.sw.out` generated from the `pynn-to-carlsim` interface is used as trace for the cycle-accurate simulator NOXIM [17]. NOXIM allows integration of circuit-level power-performance models of non-volatile memory (NVM), e.g., phase-change memory (PCM) for the crossbars and highly configurable global synapse model based on mesh architecture. The user configurable parameters include buffer size, network size, packet size, packet injection rate, routing algorithm, and selection strategy. In the power consumption simulation aspect, a user can modify the power values in external loaded YAML file to benefit from the flexibility. For the simulation results, NOXIM can calculate latency, throughput and power consumption automatically based on the statistics collected during runtime.

NOXIM has been developed using a modular structure that easily allows to add new interconnect models, which is an adoption of object-oriented programming methodology, and to experiment with them without changing the remaining parts of the simulator code. The cycle-accurate feature is provided via the SystemC programming language. This makes NOXIM the ideal framework to represent a neuromorphic hardware.

1) *Existing NOXIM Metrics:* As a traditional interconnect simulator, NOXIM provides performance metrics, which can be adopted to global synapse simulation directly. This includes:

- **Latency:** The difference between the sending and receiving time of spikes in number of cycles.
- **Network throughput:** The number of total routed spikes divided by total simulation time in number of cycles.

	<code>snn.hw.out</code>
hardware performance	specific to neuromorphic hardware latency, throughput, and energy
model performance	specific to SNN model disorder, inter-spike interval, and fanout

TABLE I: Performance metrics obtained in executing an SNN model on the neuromorphic hardware.

- **Area and energy consumption:** Area consumption is calculated based on the number of processing elements and routers; energy consumption is generated based on not only the number, but also their activation degree depending on the traffic. The area and energy consumption are high-level estimates for a given neuromorphic hardware. We adopt such high-level approach to keep the simulation speed sufficiently low, which is required to enable the early design space exploration.

2) *New NOXIM Metrics:* We introduce the following two new metrics to represent the performance impact of executing an SNN on the hardware.

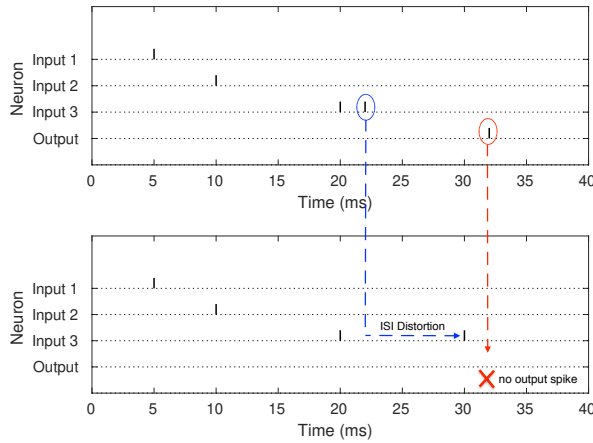
- **Disorder spike count:** This is added for SNNs where information is encoded in terms of spike frequency. The dynamic spiking frequency is calculated based on the interval of two successive spikes. The difference in the spike order between a sender and a receiver measures the amount of information loss in SNNs.
- **Inter-spike interval distortion:** Performance of supervised machine learning is measured in terms of *accuracy*, which can be assessed from inter-spike intervals (ISIs) [18]. To define ISI, we let  $\{t_1, t_2, \dots, t_K\}$  be a neuron's firing times in the time interval  $[0, T]$ . The average ISI of this spike train is given by [18]:

$$\mathcal{I} = \sum_{i=2}^K (t_i - t_{i-1}) / (K - 1). \quad (1)$$

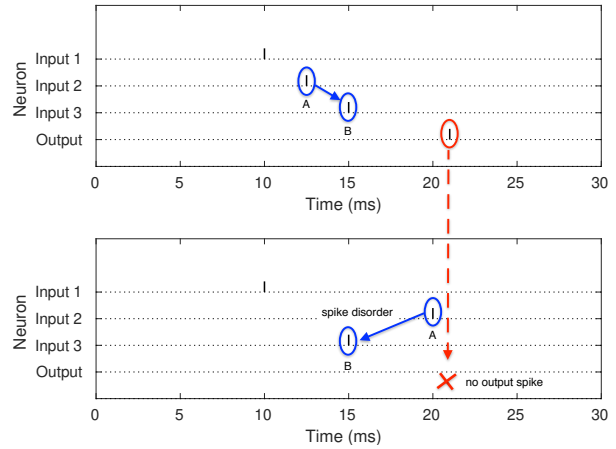
To illustrate how ISI distortion and spike disorder impact accuracy, we consider a small SNN example where three input neurons are connected to an output neuron. In Figure 17a, we illustrate the impact of ISI distortion on the output spike. In the top sub-figure, we observe that a spike is generated at the output neuron at 22ms due to spikes from the input neurons. In the bottom sub-figure, we observe that the second spike from input 3 is delayed, i.e., has ISI distortion. As a result of this distortion, there is no output spike. Missing spikes can impact application accuracy, as spikes encode information in SNNs. In Figure 17b, we illustrate the impact of spike disorder on the output spike. In the top sub-figure, we observe that the spike A from input 2 is generated before the spike B from input 3, causing an output spike to be generated at 21ms. In the bottom sub-figure, we observe that the spike order of inputs 2 and 3 is reversed, i.e., the spike B is generated before the spike A. This spike disorder results in no spike being generated at the output neuron, which can also lead to a drop in accuracy.

### B. Generating Output `snn.hw.out`

Figure 18 shows the statistics collection architecture in PyCARL. Overall, the output `snn.hw.out` consists of two performance components as highlighted in Table I.



(a) Impact of ISI distortion on accuracy. Top sub-figure shows a scenario where an output spike is generated based on the spikes received from the three input neurons. Bottom sub-figure shows a scenario where the second spike from neuron 3 is delayed. There are no output spikes generated.



(b) Impact of spike disorder on accuracy. Top sub-figure shows a scenario where spike A is received at the output neuron before spike B, causing the output spike at 21ms. Bottom sub-figure shows a scenario where the spike order of A & B is reversed. There are no output spikes generated as a result.

Fig. 17: Impact of ISI distortion (a) and spike disorder (b) on the output spike for a simple SNN with three input neurons connected to a single output neuron.

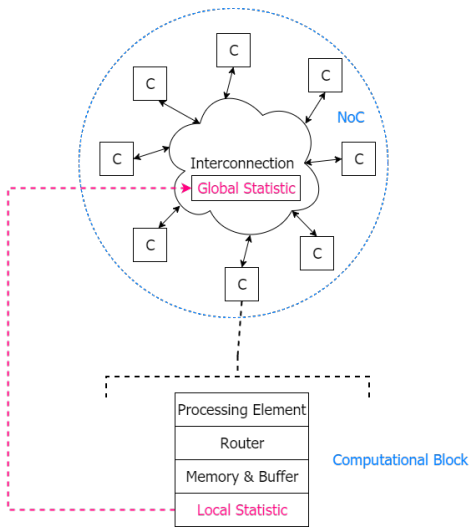


Fig. 18: Statistics collection architecture in PyCARL.

## V. EVALUATION METHODOLOGY

### A. Simulation environment

We conduct all experiments on a system with 8 CPUs, 32GB RAM, and NVIDIA Tesla GPU, running Ubuntu 16.04.

### B. Evaluated applications

Table II reports the applications that we used to evaluate PyCARL. The application set consists of 7 functionality tests from the CARLsim and PyNN repositories. The CARLsim functionality tests are testKernel{1,2,3}. The PyNN functionality tests are Izhikevich, Connections, SmallNetwork, and Varying\_Poisson. These functionalities verify the biological properties on neurons and synapses. Columns 2, 3 and 4 in the

table reports the number of synapses, the SNN topology and the number of spikes simulated by these functionality tests.

Apart from the functionality tests, we evaluate PyCARL using large SNNs for 4 synthetic and 4 realistic applications. The synthetic applications are indicated with the letter ‘S’ followed by a number (e.g., S\_1000), where the number represents the total number of neurons in the application. The 4 realistic applications are *image smoothing* (ImgSmooth) [6] on 64x64 images, *edge detection* (EdgeDet) [6] on 64x64 images using difference-of-Gaussian, *multi-layer perceptron (MLP)-based handwritten digit recognition* (MLP-MNIST) [19] on 28x28 images of handwritten digits and *CNN-based heart-beat classification* (HeartClass) [20] using ECG signals.

Category	Applications	Synapses	Topology	Spikes
functionality tests	testKernel1	1	FeedForward (1, 1)	6
	testKernel2	101,135	Recurrent (Random)	96,885
	testKernel3	100,335	FeedForward (800, 200)	63,035
	Izhikevich	4	FeedForward (3, 1)	3
	Connections	7,200	Recurrent (Random)	1,439
	SmallNetwork	200	FeedForward (20, 20)	47
	Varying_Poisson	50	FeedForward (1, 50)	700
synthetic	S_1000	240,000	FeedForward (400, 400, 100)	5,948,200
	S_1500	300,000	FeedForward (500, 500, 500)	7,208,000
	S_2000	640,000	FeedForward (800, 400, 800)	45,807,200
	S_2500	1,440,000	FeedForward (900, 900, 700)	66,972,600
realistic	ImgSmooth [6]	136,314	FeedForward (4096, 1024)	17,600
	EdgeDet [6]	272,628	FeedForward (4096, 1024, 1024, 1024)	22,780
	MLP-MNIST [19]	79,400	FeedForward (784, 100, 10)	2,395,300
	HeartClass [20]	2,396,521	CNN <sup>1</sup>	1,036,485

<sup>1</sup>. Input(82x82) - [Conv, Pool]\*16 - [Conv, Pool]\*16 - FC\*256 - FC\*6

TABLE II: Applications used for evaluating PyCARL.

## VI. RESULTS AND DISCUSSION

### A. Evaluating the proposed pyinn-carlsim interface in PyCARL

We evaluate the proposed pyinn-to-carlsim interface in PyCARL using the following two performance metrics.

- **Memory usage:** This is the amount of main memory (DDdx) occupied by each application when simulated

using PyCARL (Python). Main memory usage is reported in terms of the resident set size (in kB). Results are normalized to the native CARLsim simulation (in C++).

- **Simulation time:** This is the time consumed to simulate each application using PyCARL. Execution time is measured as CPU time (in ms). Results are normalized to the native CARLsim simulation.

1) *Memory usage:* Figure 19 plots the memory usage of each of our applications simulated using PyCARL normalized to CARLsim simulations. We make the following two observations. First, the memory usage of PyCARL is on average 3.8x higher than CARLsim. This is because 1) the pynn-carlism interface loads all shared CARLsim libraries in the main memory during initialization, irrespective of whether or not they are utilized during simulation and 2) some of CARLsim’s dynamic data structures are re-created during SWIG compilation as SWIG cannot access these native data structures in the main memory. Our future work involves solving both these limitation to reduce the memory footprint of PyCARL. Second, smaller SNNs result in higher memory overhead. This is because for smaller SNNs, the memory allocation for CARLsim libraries becomes the primary contributor of the memory overhead in PyCARL. CARLsim, on the other hand, loads only the libraries that are needed for the SNN simulation.

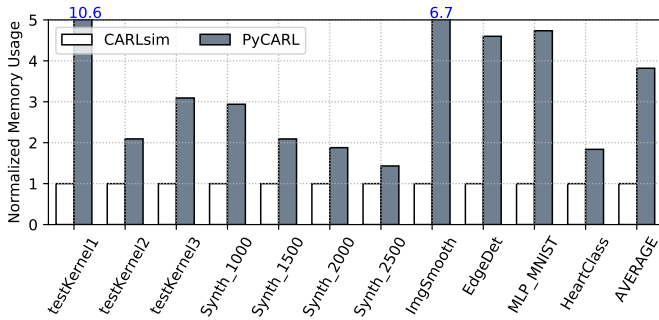


Fig. 19: Memory usage of PyCARL normalized to CARLsim (out of scale results are reported on the bar).

2) *Simulation time:* Figure 20 plots the simulation time of each of our applications using PyCARL, normalized to the simulation time using CARLsim. We make the following two observations. First, the simulation time using PyCARL is on average 4.7x higher than CARLsim. The high simulation time of PyCARL is contributed by two components – 1) initialization time, which includes the time to load all shared libraries and 2) the time for simulating the SNN. We observe that the simulation time of the SNN is comparable between PyCARL and CARLsim. The difference is in the initialization time of PyCARL, which is higher than CARLsim. Second, the overhead for smaller SNNs (i.e., ones with less number of spikes) are much higher because the initialization time dominates the overall simulation time for these SNNs, and therefore, PyCARL which has higher initialization time has much higher overall simulation time compared to CARLsim.

To analyze the simulation time, Figure 21 plots the distribution of total simulation time into initialization time and the SNN simulation time. For testKernel1 with 6 spikes (Table II), the initialization time is over 99% of the total simulation time. Since the initialization time is considerably higher in PyCARL, the overall simulation time is 17.1x than CARLsim

(see Figure 20). On the other hand, for a large SNN like Synth\_2500, the initialization time is only 8% of the total simulation time. For this application the total simulation time is only 4% higher than CARLsim.

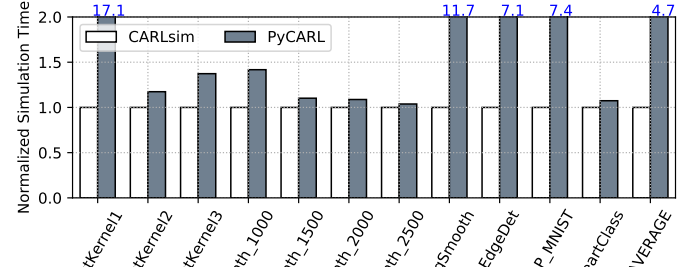


Fig. 20: Simulation time of PyCARL normalized to CARLsim (out of scale results are reported on the bar).

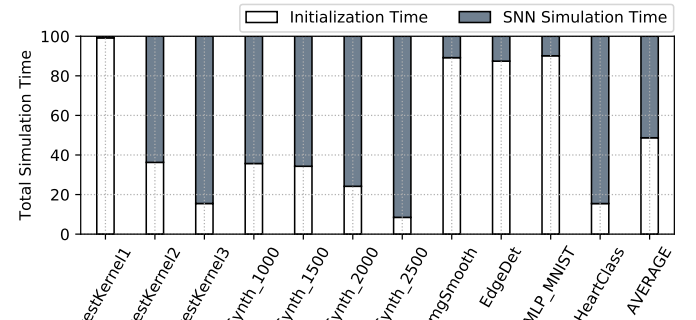


Fig. 21: Total Simulation time distributed into initialization time and SNN simulation time.

We conclude that the total simulation time using PyCARL is only marginally higher than native CARLsim for larger SNNs, which are typical in most machine learning models. This is an important requirement to enable fast design space exploration early in the model development stage. Hardware-aware circuit-level simulators are much slower and have large memory footprint. Finally, other PyNN-based SNN simulators don’t have the hardware information so they can only provide functional checking of machine learning models.

## B. Hardware-software co-simulation in PyCARL

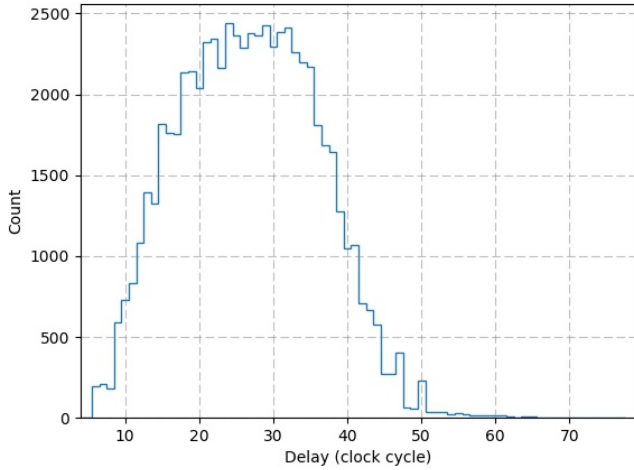
1) *Hardware configurations in PyCARL:* Table III reports the supported spike routing algorithms in PyCARL.

Algorithms	Description
XY	Packets first go horizontally and then vertically to reach destinations.
West First	West direction should be taken first if needed in the proposed route to destination.
North Last	North direction should be taken last if needed in the proposed route to destination.
Odd Even	Turning from the east at tiles located in even columns and turning to the west at tiles in odd column are prohibited.
DyAD	XY routing when there is no congestion, and Odd Even routing when there is congestion.

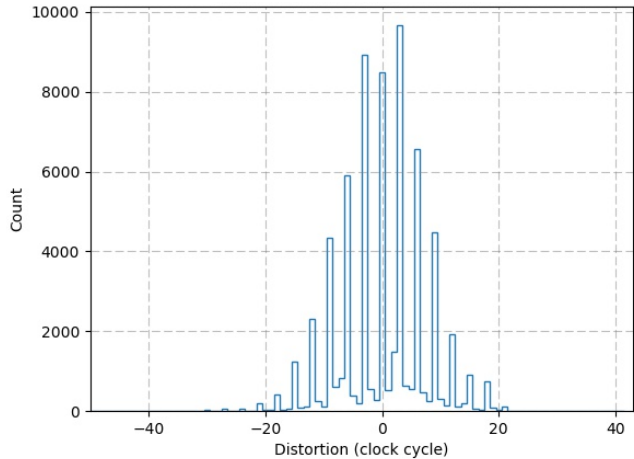
TABLE III: Routing algorithms supported in PyCARL.

To illustrate the statistics collection, we use a fully connected synthetic SNN with two feedforward layers of 18 neurons each. The SNN is mapped to a hardware with 36 crossbars arranged in a 6x6 mesh topology. Figure 22 shows a typical distribution of spike latency and ISI distortion (in clock cycles) collected when configuring the global synapse network with XY routing.





(a) Latency distribution.



(b) ISI distribution.

Fig. 22: (a) Latency and (b) ISI distortion for XY routing.

Algorithms	Avg. ISI (cycles)	Disorder Count (cycles)	Avg. Latency (cycles)	Avg. Throughput (spikes/cycle)
XY	48	203	26.75	0.191
West First	44	198	26.76	0.191
North Last	43	185	26.77	0.191
Odd Even	44	176	26.77	0.191
DyAD	44	186	26.78	0.191

TABLE IV: Evaluating routing algorithms in PyCARL.

Table IV reports the statistics collected for different routing algorithms for the global synapse network of the neuromorphic hardware. PyCARL facilitates system design exploration in the following two ways. First, system designers can explore these statistics and set a network configuration to achieve the desired optimization objective. In our prior work [21], we have developed segmented bus interconnect for neuromorphic hardware using PyCARL. Second, system designers can analyze these statistics for a given hardware to estimate performance of SNNs on hardware. In our prior work [22], we have analyzed such performance deviation using PyCARL.

2) *Performance deviation with hardware in the loop:* To illustrate how performance of a machine learning application changes for different hardware configuration, Figure 23 shows

the accuracy of the MLP\_MNIST application obtained on different hardware configurations through PyCARL compared to software-only simulation using PyNN. The configuration  $\{(n \times n) - m\}$  refers to a neuromorphic hardware with  $n^2$  crossbars, arranged using a  $n \times n$  mesh network with  $m$  being the number of inputs and outputs of each crossbar. We observe that compared to an accuracy of 89% obtained through software-based simulations, the accuracy on the  $6 \times 6$  hardware (36x crossbars with 25 neurons per crossbar) is only 66.6% – a loss of 22.4%. This loss is due to different latencies on the hardware, which delays some spikes more than others, but that is not accounted for when performing accuracy estimation through software-only simulations. PyCARL facilitates accuracy (performance in general) impact of machine learning applications, early in the development stage.

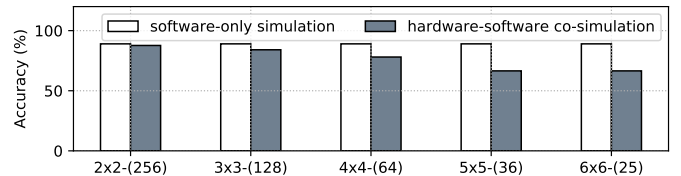


Fig. 23: Accuracy of MLP\_MNIST on different neuromorphic hardware configurations compared to the accuracy obtained via software-only simulation.

3) *SNN Performance on DynapSE:* Figure 24 evaluates the statistics collection feature of PyCARL on DynapSE [13], a state-of-the-art neuromorphic hardware to estimate performance impact between software-only simulation and hardware-software co-simulation for each of our application.

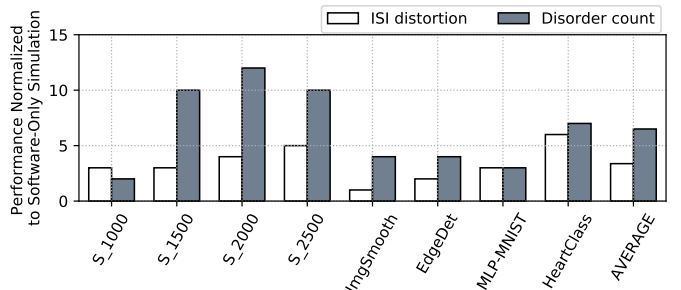


Fig. 24: ISI distortion and disorder of hardware-software co-simulation normalized to software-only simulation.

We observe that compared to software-only simulation, the hardware-software co-simulation illustrates that on average these applications have ISI distortion of 3.375 cycles and disorder of 6.5 cycles when executed on the specific neuromorphic hardware. These performance metrics directly influences performance, as illustrated in Figure 17.

4) *Design space exploration using PyCARL:* We now demonstrate how the statistics collection feature of PyCARL can be used to perform design space explorations optimizing hardware metrics such as latency and energy. We demonstrate PyCARL for DynapSE using an instance of particle swarm optimization to distribute the synapses in order to minimize latency and energy. The mapping technique is adapted from our earlier published work [22], [23]. Although optimizing SNN mapping to the hardware is not the main focus of this

paper, the following results only illustrate the capability of PyCARL to perform such optimization.

Figure 25 plots the energy and latency of each of our application normalized to PyNN, which balances the synapses on different crossbars of the hardware. We observe that PyCARL achieves an average 50% lower energy and 24% lower latency than PyNN's native load balancing strategy. These improvements clearly motivate the significance of PyCARL in advancing neuromorphic computing.

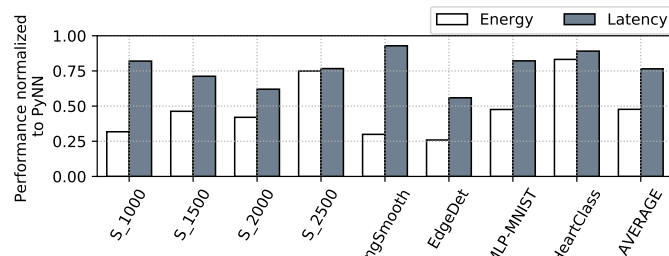


Fig. 25: Energy and latency of PyCARL normalized to PyNN.

## VII. CONCLUSIONS AND FUTURE DIRECTIONS

We present PyCARL, a Python programming interface that allows CARLsim-based spiking neural network simulations with neurobiological details at the neuron and synapse levels, co-simulations with neuromorphic hardware in the loop, and design-space explorations for neuromorphic computing, all from a common PyNN frontend. PyCARL allows extensive portability across different research institutes. We evaluate PyCARL using functionality tests as well as synthetic and realistic SNN applications on a state-of-the-art neuromorphic hardware. By using cycle-accurate models of neuromorphic hardware, PyCARL allows users to perform hardware and model explorations and performance estimation early during application development, accelerating the neuromorphic product development cycle. We **conclude** that PyCARL is a comprehensive framework that has significant potential to advance the field of neuromorphic computing.

### ACKNOWLEDGMENT

This work is supported by 1) the National Science Foundation Award CCF-1937419 (RTML: Small: Design of System Software to Facilitate Real-Time Neuromorphic Computing) and 2) the National Science Foundation Faculty Early Career Development Award CCF-1942697 (CAREER: Facilitating Dependable Neuromorphic Computing: Vision, Architecture, and Impact on Programmability).

### REFERENCES

- [1] W. Maass, "Networks of spiking neurons: the third generation of neural network models," *Neural Networks*, vol. 10, no. 9, pp. 1659–1671, 1997.
- [2] M. L. Hines and N. T. Carnevale, "The neuron simulation environment," *Neural Computation*, vol. 9, no. 6, pp. 1179–1209, 1997.
- [3] M.-O. Gewaltig and M. Diesmann, "Nest (neural simulation tool)," *Scholarpedia*, vol. 2, no. 4, p. 1430, 2007.
- [4] D. Pecevski, T. Natschläger, and K. Schuch, "Pcsim: a parallel simulation environment for neural circuits fully integrated with python," *Frontiers in Neuroinformatics*, vol. 3, p. 11, 2009.
- [5] D. F. Goodman and R. Brette, "Brian: a simulator for spiking neural networks in python," *Frontiers in Neuroinformatics*, vol. 2, p. 5, 2008.
- [6] T.-S. Chou, H. J. Kashyap, J. Xing, S. Listopad, E. L. Rounds, M. Beyeler, N. Dutt, and J. L. Krichmar, "Carlsim 4: an open source library for large scale, biologically detailed spiking neural network simulation using heterogeneous clusters," in *International Joint Conference on Neural Networks (IJCNN)*. IEEE, 2018, pp. 1–8.

- [7] J. M. Nageswaran, N. Dutt, J. L. Krichmar, A. Nicolau, and A. V. Veidenbaum, "A configurable simulation environment for the efficient simulation of large-scale spiking neural networks on graphics processors," *Neural Networks*, vol. 22, no. 5-6, pp. 791–800, 2009.
- [8] A. P. Davison, D. Brüderle, J. M. Eppler, J. Kremkow, E. Müller, D. Pecevski, L. Perrinet, and P. Yger, "PyNN: a common interface for neuronal network simulators," *Frontiers in Neuroinformatics*, vol. 2, p. 11, 2009.
- [9] J. M. Eppler, M. Helias, E. Müller, M. Diesmann, and M.-O. Gewaltig, "PyNEST: a convenient interface to the NEST simulator," *Frontiers in Neuroinformatics*, vol. 2, p. 12, 2009.
- [10] D. Pecevski, T. Natschläger, and K. Schuch, "PCSIM: a parallel simulation environment for neural circuits fully integrated with Python," *Python in Neuroscience*, p. 61, 2015.
- [11] S. Marcel and B. Romain, "Brian 2, an intuitive and efficient neural simulator," *eLife*, vol. 8, 2019.
- [12] C. Mead, "Neuromorphic electronic systems," *Proceedings of the IEEE*, vol. 78, no. 10, pp. 1629–1636, 1990.
- [13] S. Moradi, N. Qiao, F. Stefanini, and G. Indiveri, "A Scalable Multicore Architecture with Heterogeneous Memory Structures for Dynamic Neuromorphic Asynchronous Processors (DYNAPs)," *IEEE Transactions on Biomedical Circuits and Systems*, vol. 12, no. 1, pp. 106–122, 2018.
- [14] M. V. DeBole, B. Taba, A. Amir, F. Akopyan, A. Andreopoulos, W. P. Risk, J. Kusnitz, C. O. Otero, T. K. Nayak, R. Appuswamy *et al.*, "Truenorth: Accelerating from zero to 64 million neurons in 10 years," *Computer*, vol. 52, no. 5, pp. 20–29, 2019.
- [15] M. Davies, N. Srinivasa, T.-H. Lin, G. Chinya, Y. Cao, S. H. Choday, G. Dimou, P. Joshi, N. Imam, S. Jain *et al.*, "Loihi: A neuromorphic manycore processor with on-chip learning," *IEEE Micro*, vol. 38, no. 1, pp. 82–99, 2018.
- [16] E. M. Izhikevich, "Simple model of spiking neurons," *IEEE Transactions on Neural Networks*, vol. 14, no. 6, pp. 1569–1572, 2003.
- [17] V. Catania, A. Mineo, S. Monteleone, M. Palesi, and D. Patti, "Noxim: An open, extensible and cycle-accurate network on chip simulator," in *International Conference on Application-specific Systems, Architectures and Processors (ASAP)*. IEEE, 2015, pp. 162–163.
- [18] S. Grün and S. Rotter, *Analysis of parallel spike trains*. Springer, 2010, vol. 7.
- [19] P. U. Diehl and M. Cook, "Unsupervised learning of digit recognition using spike-timing-dependent plasticity," *Frontiers in Computational Neuroscience*, vol. 9, p. 99, 2015.
- [20] A. Balaji, F. Corradi, A. Das, S. Pande, S. Schaafsma, and F. Catthoor, "Power-accuracy trade-offs for heartbeat classification on neural networks hardware," *Journal of Low Power Electronics*, vol. 14, no. 4, pp. 508–519, 2018.
- [21] A. Balaji, Y. Wu, A. Das, F. Catthoor, and S. Schaafsma, "Exploration of segmented bus as scalable global interconnect for neuromorphic computing," in *Proceedings of the Great Lakes Symposium on VLSI*. ACM, 2019, pp. 495–499.
- [22] A. Das, Y. Wu, K. Huynh, F. Dell'Anna, F. Catthoor, and S. Schaafsma, "Mapping of local and global synapses on spiking neuromorphic hardware," in *Conference on Design, Automation & Test in Europe*. IEEE, 2018, pp. 1217–1222.
- [23] A. Balaji, A. Das, Y. Wu, K. Huynh, F. G. Dell'Anna, G. Indiveri, J. L. Krichmar, N. D. Dutt, S. Schaafsma, and F. Catthoor, "Mapping spiking neural networks to neuromorphic hardware," *IEEE Transactions on Very Large Scale Integration (VLSI) Systems*, vol. 28, no. 1, pp. 76–86, 2019.